Title:

Mitochondrial DNA has strong selective effects across the nuclear genome

Authors:

Timothy M. Healy and Ronald S. Burton

Marine Biology Research Division, Scripps Institution of Oceanography, University of California San Diego, 9500 Gilman Drive #0202, La Jolla, CA, USA

Abstract:

Oxidative phosphorylation requires gene products encoded in both the nuclear and mitochondrial genomes, and is the primary source of cellular energy in eukaryotes. As a result, functional integration between the genomes is essential for efficient ATP generation in these organisms. Although within populations this integration is presumably maintained by coevolution, both the importance of coevolution in speciation and mitochondrial disease, and the strength of selection for maintenance of coevolved genotypes are widely questioned. In this study, we crossed populations of the intertidal copepod, *Tigriopus californicus*, to disrupt putatively coevolved mitonuclear genotypes in reciprocal F_2 hybrids. We utilized inter-individual variation in developmental rate, a proxy for fitness, among these hybrids to assess the strength of selection imposed on the nuclear genome by alternate mitochondrial genotypes. There was substantial variation in developmental rate among hybrid individuals, and *in vitro* ATP synthesis rates of mitochondria isolated from high fitness hybrids were approximately twice those of mitochondria isolated from low fitness individuals. Furthermore, we used Pool-seq to reveal large deviations in nuclear allele frequencies in hybrids, which favored maternal alleles in only high fitness individuals of each reciprocal cross. Therefore, our most fit hybrids had partial recovery of coevolved genotypes, indicating that mitonuclear effects underlie individual-level variation in developmental rate and that inter-genomic compatibility is critical for high fitness. These results demonstrate that mitonuclear interactions have profound impacts on both physiological performance and the evolutionary trajectory of the nuclear genome.

Introduction:

Oxidative phosphorylation in the mitochondria is central to the functioning of essentially all eukaryotic cells, and thus is critical for the majority of complex life (Rand et al., 2004; Lane, 2005; Wallace, 2010a; Hill, 2015). Over evolutionary time most mitochondrial genes have translocated to the nucleus, but a small number that are necessary for ATP generation are still encoded within the mitochondria: typically 13 protein coding, 2 rRNA and 22 tRNA genes in bilaterian animals (Levin et al., 2014). These genes require functional interactions with nuclear-encoded proteins, and thus mitochondrial performance relies upon integration between the nuclear and mitochondrial genomes (Rand et al., 2004; Lane, 2005; Hill, 2015). Consequently, there is predicted to be strong selection for mitonuclear compatibility between interacting genes (i.e., coevolution) in isolated populations and species (Sloan et al., 2017; Hill et al., 2018).

Despite the likelihood of strong selection for compatible mitonuclear genotypes, coevolved mitochondrial and nuclear genes may be disassociated by hybridization when isolated populations experience secondary contact (Burton & Barreto, 2012). Mismatches between mitochondrial-encoded and nuclear-encoded alleles can have profound negative phenotypic consequences across many traits (i.e., hybrid breakdown), ranging from diseases in humans (Wallace, 2010b) to life-history effects in invertebrates (Burton, 1990; Ellison & Burton, 2008b; Meiklejohn et al., 2013). These examples of Bateson-Dobzhansky-Muller incompatibilities (Bateson, 1909; Dobzhansky, 1937; Muller, 1942) may have important implications for post-zygotic isolation between species (Gershoni et al., 2009; Hill, 2016, 2019), and mitochondrial replacement therapies in humans (Reinhardt et al., 2013). However, the ubiquity and relevance of these implications have

been questioned for humans specifically (Eyre-Walker, 2017), and for eukaryotes generally (Sloan et al., 2017). Therefore, determining the extent to which mitonuclear interactions influence evolution of the nuclear genome, and the degree to which inter-genomic incompatibilities result in negative fitness consequences are critical for understanding the role of mitochondrial DNA in shaping the physiological performance and evolution of eukaryotes.

In the current study, we address these issues using hybrids between a San Diego, CA (SD) and a Santa Cruz, CA (SC) population of the intertidal copepod *Tigriopus californicus*. This species is found in supralittoral tidepools along the west coast of North America from Baja California, Mexico to Alaska, USA with extremely low gene flow between isolated populations on different rocky outcrops (Burton, 1997). This isolation has led to high levels of genetic divergence among populations (Burton & Lee, 1994; Burton 1997; Edmands, 2001; Peterson et al., 2013; Pereira et al., 2016 Barreto et al., 2018), and F_2 hybrids from inter-population laboratory crosses typically display breakdown of mitochondrial ATP synthesis capacities and several fitness-related life-history traits, including fecundity and developmental rate (Burton, 1990; Edmands, 1999; Ganz & Burton, 1995; Ellison & Burton, 2008b, Burton et al., 2006). This loss of performance is recovered by backcrossing hybrids to the maternal, but not the paternal, parental population (Ellison & Burton, 2008b), which, since mitochondrial DNA is maternally inherited (Burton & Barreto, 2012), clearly implicates a role for mitonuclear interactions in hybrid breakdown in this species. Here, we reasoned that if there is strong selection for mitonuclear matching throughout ontogeny (Hill et al., 2018), then there should be clear physiological and genetic associations with variation in fitness-related

traits among F_2 hybrids. Thus, we utilized inter-individual differences in developmental rate and ATP synthesis rate in combination with Pool-seq to assess the importance of, and strength of selection for, coevolved mitonuclear genomes in eukaryotes.

Materials and methods:

Copepod collection and culturing

Adult copepods were collected with fine-mesh dip nets and large plastic pipettes from splashpools near San Diego, CA (SD; 32° 45′ N, 117° 15′ W) and Santa Cruz, CA (SC; 36° 56′ N, 122° 02′ W) in the spring of 2018. Collected animals were transported back to Scripps Institution of Oceanography in 1 L plastic bottles containing water collected from the tidepools. Collections were split into approximately fifteen 200 mL laboratory cultures that were established in 400 mL glass beakers, and held across four incubators for laboratory acclimations. Acclimation conditions (20 °C, 36 ppt and 12:12 light:dark) were maintained for at least one month (approximately one generation) prior to the start of all experiments. Copepods consumed natural algal growth in the cultures as well as a mixture of ground fish flakes and powdered Spirulina that were fed to each culture ad lib.

Inter-population crosses

Prior to mating, male *T. californicus* clasp juvenile females forming a breeding pair (Burton, 1985). Females mate only once, and thus separation of precopulatory breeding pairs allows the isolation of virgin females for experimental crosses (Burton, 1985). Two sets of reciprocal crosses were made between SD and SC copepods. First, for assessment of variation in ATP synthesis rates (see below), 40 pairs of each population were gently teased apart with a needle (e.g., Burton et al., 1981), and males of one

106 population were combined with females of the other population in 10 cm petri dishes
107 containing ~60 mL of filtered seawater. Copepods were allowed to pair, and the dishes
108 were monitored for the appearance of gravid females, which, when observed, were
109 moved to a new dish. These females were allowed to produce multiple egg sacs each in
110 the new dish, and were removed once F_1 offspring were visible. F_1 offspring matured and
111 haphazardly formed breeding pairs. Gravid females were again moved to a new dish, and
112 were monitored until mature (red) F_2 egg sacs were observed. Second, for isolation of
113 DNA for Pool-seq (see below), 120 pairs of each population were separated, and
114 reciprocal F_2 hybrid egg sacs were obtained as described above. Throughout the
115 experimental crosses holding conditions and feeding routines were the same as those for
116 the initial laboratory acclimations.

117 *Inter-individual variation in developmental time*

118 Variation in developmental rate among individuals was assessed for both parental
119 and F_2 hybrid copepods by measurement of time to metamorphosis (e.g., Harada et al.,
120 2019). *T. californicus* development consists of 6 naupliar stages, 5 copepodid stages and
121 the final adult stage (Tsuboko-Ishii & Burton, 2018). The majority of stages are visually
122 cryptic; however, there is a substantial metamorphosis between the final naupliar stage
123 and initial copepodid stage (i.e., copepodid stage I), which can be observed through a
124 microscope. To score inter-individual differences in developmental rate, gravid females
125 with red egg sacs were pipetted onto filter paper, egg sacs were removed with a fine
126 needle, and dissected egg sacs were placed in filtered seawater in 6-well plates (≤ 4 per
127 well). This procedure synchronizes hatching as dissected mature egg sacs hatch
128 overnight. Offspring were fed Spirulina, and were monitored daily for the appearance of

129 copepodids. Days post hatch (dph) to metamorphosis was scored for all individuals, and
130 copepodids were moved to fresh petri dishes after scoring. In total, offspring from 68 SD
131 egg sacs, 58 SC egg sacs, 352 F_2 SD♀xSC♂ egg sacs (205 for ATP assays and 147 for
132 Pool-seq) and 314 F_2 SC♀xSD♂ egg sacs (115 for ATP assays and 199 for Pool-seq)
133 were scored.

134 *ATP synthesis rates*

135 F_2 hybrid copepodids were divided into four developmental time groups: 8-10,
136 11-13, 14-16 and ≥17 dph to metamorphosis. Development was allowed to continue, and
137 adults from the 8-10, 11-13 and ≥17 dph groups were used for assessment of maximal
138 mitochondrial ATP synthesis rates as in Harada et al. (2019). In brief, for each reciprocal
139 cross, 6 pools of 6 adults from each developmental group were moved to petri dishes with
140 fresh filtered seawater and no food overnight. Each pool of copepods was then
141 homogenized in 800 µL of ice-cold homogenization buffer (400 mM sucrose, 100 mM
142 KCl, 70 mM HEPES, 3 mM EDTA, 6 mM EGTA, 1% BSA, pH 7.6) in 1 mL teflon-on-
143 glass homogenizers. Homogenates were transferred to 1.5 mL microcentrifuge tubes, and
144 centrifuged at 1,000 g for 5 min at 4 °C. Supernatants were pipetted to new 1.5 mL tubes,
145 which were then centrifuged at 11,000 g for 10 min at 4 °C. After removal of the
146 supernatants, mitochondrial pellets were resuspended in 55 µL of assay buffer (560 mM
147 sucrose, 100 mM KCl, 70 mM HEPES, 10 mM KH_2PO_4, pH 7.6). For the ATP synthesis
148 assays, 5 µL of a complex I substrate cocktail (final assay substrate concentrations: 5 mM
149 pyruvate, 2 mM malate and 1 mM ADP) was added to 25 µL of each sample in 0.2 mL
150 strip tubes. This was done twice for each sample: once for the initial ATP concentration
151 determinations and once for the ATP synthesis reactions. For initial ATP measurements,

CellTiter-Glo (Promega, Madison, WI), which is used for ATP quantification and prevents additional ATP synthesis, was immediately added to one tube for each sample after substrate additions. For synthesis reactions, the second tube for each sample was incubated at 20 °C for 10 min prior to the addition of CellTiter-Glo. All samples were incubated with CellTiter-Glo at room temperature in the dark for 10 min prior to reading luminescence with a Fluoroskan Ascent® FL (Thermo Fisher Scientific, Waltham, MA). Sample luminescence was compared to an ATP standard curve, and ATP synthesis rate was calculated by subtracting initial ATP concentrations from final ATP concentrations. Protein content in each sample was measured with NanoOrange Protein Quantification Kits according to the manufacturer's instructions (Thermo Fisher Scientific, Waltham, MA), and was used for ATP synthesis rate normalization. Variation in synthesis rates among groups was assessed by two-way ANOVA with cross and developmental time as factors followed by Tukey post-hoc tests in R v3.4.0 (The R Foundation, Vienna, Austria).

Genomic sequencing and allele frequency determination

Two developmental groups of F_2 hybrid copepodids for each reciprocal cross were allowed to develop to adulthood: those that metamorphosed 8-12 dph ("fast developers") and those that metamorphosed >22 dph ("slow developers"). For each group, 180 adults (approximately equal numbers of females and males) were pooled for DNA isolation by phenol-chloroform extraction (Sambrook & Russell, 2006). Briefly, copepods were rinsed with deionized water and homogenized by hand in 150 µL of Bender buffer (200 mM sucrose, 100 mM NaCl, 100 mM Tris-HCl pH 9.1, 50 mM EDTA, 0.5% SDS) in 1.5 mL microcentrifuge tubes. An additional 250 µL of Bender

buffer was added to each sample followed by 100 µg of Proteinase K (Thermo Fisher Scientific, Waltham, MA). Samples were incubated at 56 °C overnight then cooled to room temperature for ~15 min. 25 µg of RNase A (Thermo Fisher Scientific, Waltham, MA) was added to each sample prior to a 37 °C incubation for 30 min, which was followed by addition of 200 µL of 5M potassium acetate and a 10 min incubation on ice. Samples were then centrifuged at 13,000 g for 10 min at 4 °C, supernatants were transferred to 2.0 mL microcentrifuge tubes, and 400 µL of UltraPure™ Buffer-Saturated Phenol (Thermo Fisher Scientific, Waltham, MA) and 400 µL of OmniPur® Chloroform (EMD Millipore Corporation, Darmstadt, Germany) were added to each supernatant. The phenol-chloroform mixtures were then gently mixed for 1 min, and centrifuged at 20,000 g for 5 min at 4 °C. Aqueous phases were transferred to new 2.0 mL tubes, and organic phases were back-extracted as above to maximize DNA yield. 400 µL of chloroform was again added to each aqueous phase for re-extraction: samples were centrifuged at 15,000 g for 1 min at 4 °C, aqueous phases were transferred to new 2.0 mL tubes, and again organic phases were back-extracted repeating the above procedure. 1,200 µL of ice-cold 95% ethanol was added to each aqueous phase; tubes were incubated at -20 °C for 1 h to facilitate DNA precipitation, and then centrifuged at 16,000 g for 20 min at 4 °C. 95% ethanol was removed by pipette, and all pellets for a sample (from back-extractions etc.) were combined in 1,000 µL of ice-cold 75% ethanol. Samples were then centrifuged at 16,000 g for 5 min at 4 °C. 75% ethanol was removed by pipette followed by an additional 16,000 g centrifugation for 1 min at 4 °C. Any remaining ethanol was removed and samples were dried in air for 20 min then resuspended in UltraPure™ Distilled Water (Thermo Fisher Scientific, Waltham, MA). DNA isolations were quantified with a

198 Qubit® 2.0 Fluorometer and a dsDNA HS assay kit according to the manufacturer's
199 instructions (Thermo Fisher Scientific, Waltham, MA).
200 Approximately 1 μg of genomic DNA for each pool was sent to Novogene Co.,
201 Ltd. (Sacramento, CA) for whole-genome 150 bp paired-end sequencing on a NovaSeq
202 6000 (Illumina Inc., San Diego, CA). Between 59,765,048 and 74,464,410 paired reads
203 were obtained for each sample, which were trimmed to remove adapter sequences and
204 base pairs with Phred scores less than 25. After trimming, reads with less than 50 bp
205 remaining were removed. BWA MEM v0.7.12 (Li & Durbin, 2009) was used to align the
206 filtered reads to the SD *T. californicus* reference genome v2.1 (Barreto et al., 2018) and
207 an updated SC reference genome, which was prepared as described in Barreto et al.
208 (2018) and Lima et al. (2019). Prior to read mapping the references were equalized such
209 that any "N" position in one reference was also an "N" in the other reference. Mapping
210 hybrid sample reads to both parental references allows calculation of average allele
211 frequency estimates between the mappings, which accounts for mapping biases between
212 matched and mismatched allelic reads (Lima & Willett, 2018). Read mappings with
213 MAPQ scores less than 20 were discarded, resulting in average genome coverage values
214 between 65X and 83X for all sample-to-reference combinations (Tables 1, 2). 2,768,859
215 biallelic single nucleotide polymorphisms (SNPs) that are fixed between the SD and SC
216 populations were identified using the previously published methods (Lima & Willett,
217 2018; Lima et al., 2019) with population-specific sequencing reads obtained from Barreto
218 et al. (2018). Briefly, population-specific reads were mapped to the other population's
219 reference genome, and variant loci with minor allele frequencies of 0 in both mappings
220 were kept as fixed inter-population SNPs. Sample allele frequencies at these SNPs were

221 determined using PoPoolation2 (Kofler et al., 2011) for all sites that had a minimum
222 coverage of at least 4 for the minor allele in the mappings to both parental reference
223 genomes (as in Lima et al., 2019). Estimated allele frequencies for each sample were
224 averaged between the two mappings to account for mapping biases, and mean allele
225 frequencies were calculated for non-overlapping 250 kb windows along each
226 chromosome, which reduces noise in allele frequency estimates as a single generation of
227 recombination between SD and SC chromosomes (which occurs only in males in *T.*
228 *californicus* [Burton et al., 1981]) is not expected to break apart large chromosomal
229 blocks in F_2 hybrids (Lima & Willett, 2018).

230 Deviations in F_2 allele frequencies associated with mitonuclear effects between
231 fast and slow developers were detected for each cross as in Lima et al. (2019). First,
232 average maternal allele frequencies were calculated for non-overlapping 2 Mb blocks
233 along each chromosome (7-9 blocks per chromosome), and Kolmogorov-Smirnov (KS)
234 tests in R v3.4.0 were used to assess if the allele frequencies across each chromosome in
235 each pool were drawn from the same distribution. False-discovery rate associated with
236 multiple tests was accounted for by Bonferroni correction of $\alpha = 0.05$. Second, for
237 chromosomes with significant KS test results, the tenth ($q_{0.1}$) and ninetieth ($q_{0.9}$) quantiles
238 of the allele frequencies calculated over 250 kb blocks were compared between fast and
239 slow developers. Lack of overlap between the quantiles is consistent with a potential
240 mitonuclear effect on developmental rate. These potential effects were then resolved by
241 comparisons between the reciprocal crosses; higher maternal allele frequencies in the fast
242 developers than the slow developers in both reciprocals or in one reciprocal with no allele
243 deviations in the other reciprocal are consistent with effects of mitonuclear matching. In

244 contrast, higher paternal alleles frequencies in fast developers using the same
245 comparisons are consistent with mitonuclear mismatching. Third, allele frequency
246 deviations greater than or equal to ±0.05 were identified, as this minimum deviation has
247 been suggested as a threshold for chromosomal regions most likely to contain genes
248 involved in mitonuclear effects using these methods (Lima & Willett, 2018). These
249 analyses were repeated comparing SD allele frequencies between the reciprocal crosses
250 for the fast and slow pools separately as an alternative test of allele deviations consistent
251 with mitonuclear incompatibilities. In fast developers, greater frequencies of the SD allele
252 in the SD♀xSC♂ than the SC♀xSD♂ cross are consistent with effects of mitonuclear
253 matching. In contrast, expected patterns in slow developers are more challenging to
254 predict. For example, lower frequencies of the SD allele in the slow developing
255 SD♀xSC♂ copepods than in the slow developing SC♀xSD♂ copepods would be
256 consistent with effects of mitonuclear incompatibilities. However, because different sites
257 of mismatches could independently cause similar negative phenotypic effects and
258 individuals with many mismatches might be expected to fail development at early stages,
259 it is also possible that few allelic deviations would be expected in slow developers even if
260 mitonuclear interactions affected developmental rate. Finally, effects of nuclear genetic
261 variation alone were assessed by determining the chromosomes for which allele
262 frequencies deviated in the same direction from 0.5 in both fast developing reciprocal
263 pools or both slow developing reciprocal pools, such that $q_{0.1}$ and $q_{0.9}$ did not overlap
264 with 0.52 or 0.48 in either reciprocal. These boundaries are likely conservative quantile
265 limits for neutral variation in allele frequency estimates using these methods (Lima &
266 Willett, 2018; Lima et al., 2019).

Results:

Developmental rates were similar in both parental populations of *T. californicus* with metamorphosis occurring approximately 8-22 days post hatch (dph) for ~98% of nauplii (maximum dph of 29 and 24 for SD and SC, respectively; Fig. 1A). In contrast, the distributions of developmental time among F_2 hybrids from both reciprocal crosses demonstrated a substantial skew favoring higher dph to metamorphosis compared to the parental populations, which is consistent with hybrid breakdown (Fig. 1B). In both crosses, metamorphosis was observed 8-30 dph with 8 out of 473 SD♀xSC♂ nauplii and 245 out of 1,242 SC♀xSD♂ nauplii still present on day 30, which were scored as >30 dph. Preliminary data suggested that the majority of nauplii underwent metamorphosis 9-16 dph, and thus F_2 hybrids were split into 8-10, 11-13 and ≥17 dph groups to assess maximal ATP synthesis rates. Complex I-fueled ATP synthesis rates were significantly affected by both cross ($F_{1,30} = 11.32$; $P = 2.1 \times 10^{-3}$) and developmental group ($F_{2,30} = 13.44$; $P = 6.8 \times 10^{-5}$) with no interaction between factors ($F_{2,30} = 0.44$; $P = 0.65$), and post-hoc tests indicated that 8-10 dph copepods had higher ATP synthesis rates than ≥17 dph copepods in both crosses ($P \leq 0.04$; Fig. 1C). In SC♀xSD♂ hybrids, 11-13 dph copepods had ATP synthesis rates that were similar to those of 8-10 dph copepods ($P = 0.52$) and higher than those of ≥17 dph copepods ($P = 0.01$). In contrast, 11-13 dph SD♀xSC♂ copepods had intermediate synthesis rates compared to 8-10 and ≥17 dph copepods ($P \geq 0.13$ for both comparisons; Fig. 1C).

F_2 hybrids from a second set of reciprocal crosses were divided into those that metamorphosed 8-12 or >22 dph (fast or slow developers, respectively) to assess parental allele frequency deviations associated with variation in developmental rate. When

290 considering all 2,768,859 SNPs that were fixed between the SD and SC populations,
291 there were shifts towards higher maternal allele frequencies in fast developers, and higher
292 paternal allele frequencies in slow developers in each reciprocal cross (Fig. 2). Biases
293 towards maternal alleles in fast developers became particularly evident when allele
294 frequencies were examined across chromosomes (Fig. 3), as in both reciprocal crosses
295 there were significant frequency shifts favoring coevolved alleles in fast developers
296 across large regions of chromosomes 1, 3, 4 and 5 ($P \leq 5.8 \times 10^{-4}$; Figure 3A). Although
297 deviations within a single reciprocal could be consistent with nuclear-only effects, the
298 observation of maternal biases in both crosses clearly suggests involvement of
299 mitonuclear interactions. Patterns consistent with mitonuclear effects were also detected
300 for chromosomes 2 and 8 in SC♀xSD♂ hybrids, as there were biases for SC alleles in
301 fast developers in this cross ($P = 5.8 \times 10^{-4}$ for both; Fig. 3B), and these alleles were not
302 favored in fast developing SD♀xSC♂ hybrids. Additionally, there were significant
303 potential mitonuclear effects on chromosomes 7 and 12 in the SC♀xSD♂ cross ($P \leq 1.6 \times$
304 10^{-4} for both; Fig. 3B); however, these patterns were subtle relative to those on other
305 chromosomes. On chromosome 7, SC alleles were more common in fast than in slow
306 developers, but SC allele frequencies did not exceed 0.5 in either pool, and on
307 chromosome 12, trends in allele frequencies suggested a similar pattern to the one
308 observed on chromosome 7, but quantile overlap comparisons did not conclusively
309 resolve the direction of this potential effect. In general, comparisons between the
310 reciprocal crosses for fast or slow developers demonstrated similar mitonuclear effects to
311 those describe above, and there were no clear nuclear-only effects for any chromosome
312 (Fig. 4). Furthermore, these comparisons detected biases for paternal (i.e., mismatched)

313 nuclear alleles in slow developers (for chromosomes 1, 3, 4, 7 and 12; Fig. 4). Despite the
314 overall association between high fitness and coevolved mitonuclear genotypes in our
315 study, allele frequencies across one chromosome in each reciprocal were consistent with
316 the opposite effect as excess paternal alleles were observed in fast developers
317 (chromosome 6 for SD♀xSC♂ and chromosome 11 for SC♀xSD♂; Fig. 3). Yet, taken
318 together these results suggest that mitonuclear interactions are the major genetic factors
319 contributing to inter-individual variation in developmental rate among F_2 hybrids, and
320 that in the majority of cases at least partial maintenance of coevolved mitonuclear
321 genotypes is critical for performance in this fitness-related trait.

322 **Discussion:**

323 Mitochondrial DNA contains relatively few genes, but because of the functional
324 products encoded by these genes and their interactions with nuclear gene products,
325 differences in mitochondrial genotype are predicted to exert strong selection pressures on
326 the nuclear genome throughout ontogeny (Hill et al., 2018). In the current study, we
327 demonstrate substantial consequences of mitonuclear interactions on developmental rate,
328 ATP synthesis rate, and nuclear allele frequencies in hybrids that are consistent with
329 strong selection for compatible interactions within even a single generation. In our
330 reciprocal crosses, coevolved nuclear alleles that matched alternate mitochondrial
331 genotypes were favored on at least four of the twelve chromosomes in high fitness F_2
332 hybrids. Relative to previous studies in *T. californicus* hybrids (Pritchard et al., 2011;
333 Foley et al., 2013; Lima et al., 2019), this clear pattern towards partial recovery of
334 coevolved mitonuclear genotypes is most likely a consequence of selecting individuals
335 based on variation in a fitness-related trait that has been correlated with mitochondrial

336 performance in this species (Ellison & Burton, 2006). Average chromosome-wide allele
337 frequency deviations favoring coevolved alleles ranged from 0.033 to 0.109 with some
338 regions favoring these alleles by ~0.138 (Figs. 3, 4). F_1 hybrids between SD and SC
339 (heterozygous across all fixed SNPs) generally show enhanced fitness compared to
340 parentals (Ellison & Burton, 2008b), and there is little evidence for selection against
341 heterozygous F_2 hybrids (Pritchard et al., 2011; Foley et al., 2013). Therefore, it is likely
342 that the major allele frequency deviations in the current study are consequences of
343 negative effects associated with one of the two possible homozygous genotypes. As a
344 result, given Mendelian segregation ratios of 1:2:1, the most extreme biases for maternal
345 alleles in our study are likely indicative of approximately 67-87% deficits of homozygous
346 paternal genotypes in fast developing F_2 hybrids on some regions of these chromosomes.
347 Thus, our data demonstrate strong selection favoring mitonuclear compatibility.
348 Additionally, despite previous detection of nuclear-only effects on intrinsic selection for
349 survival in *T. californicus* hybrids (Lima et al., 2019), we observed no clear allele
350 frequency deviations consistent with nuclear-only effects on developmental rate, which
351 also suggests that mitonuclear incompatibilities are key genetic mechanisms resulting in
352 loss of fitness in these hybrids.

353 Previous studies have demonstrated at least three candidate mechanisms involved
354 in coevolution in *T. californicus*: electron transport system complex activities (Willett &
355 Burton, 2001, 2003; Rawson & Burton, 2002; Harrison & Burton, 2005; Ellison &
356 Burton, 2008b), mitochondrial transcription (Ellison & Burton, 2008a) and mitonuclear
357 ribosomal interactions (Barreto & Burton, 2012). Yet, these studies do not directly reveal
358 the number or relative importance of mitonuclear incompatibilities contributing to hybrid

359 breakdown in this species. In comparison, our Pool-seq approach resolves essentially the
360 full genomic architecture of breakdown of developmental rate in hybrids between SD and
361 SC. The substantial biases for maternal alleles across multiple genomic regions in our
362 most fit hybrids clearly indicate a polygenic basis for mitonuclear coevolution, which
363 may be attributable to the high level of divergence between the mitochondrial genomes of
364 these populations (21.7%; Barreto et al., 2018). However, because of the mitochondrion's
365 central role in metabolism, even minor disruption of mitonuclear interactions can have
366 major fitness effects (Burton & Barreto, 2012, Hill et al., 2018). For example, mutations
367 in a single nuclear-encoded mitochondrial tRNA synthetase and one mitochondrial tRNA
368 lead to mitochondrial dysfunction in *Drosophila* hybrids (Meiklejohn et al., 2013). The
369 allele frequency variation in our slow developing hybrids is likely consistent with large
370 effects of few interactions in *T. californicus* as well. Despite an approximately two-fold
371 reduction in both developmental rate and ATP synthesis rate (Fig. 1), strong deviations
372 favoring paternal alleles in slow developers were largely absent in our study (with the
373 exception of chromosome 4 in SD♀xSC♂; Figs. 3, 4). Consequently, our data suggest
374 that for any given individual, relatively few incompatible interactions are necessary to
375 result in substantial negative fitness effects.

376 Of the 1,000-1,500 nuclear-encoded mitochondrial (N-mt) genes in metazoans, at
377 least 180 are expected to have intimate functional interactions with either mitochondrial
378 DNA or mitochondrial-encoded gene products (N_O-mt genes) (Burton et al., 2013).
379 Barreto et al. (2018) identified 599 putative N-mt genes, including 139 N_O-mt genes, in
380 the *T. californicus* genome (Figs. 3C, 4C). Although our data begin to resolve which of
381 these candidates may play the largest roles in inter-genomic coevolution, there was little

382 resolution of allele frequency deviations beyond the level of chromosomes in our hybrids.
383 This is likely a consequence of only a single opportunity for inter-population
384 recombination in F_2 hybrids (Lime & Willett, 2018), or involvement of multiple loci
385 within the same chromosome (Willett et al., 2016). Although N-mt genes were not more
386 common on the chromosomes with biases for coevolved alleles than on other
387 chromosomes in our study, chromosomes demonstrating allelic biases tended to have
388 relatively higher ratios of N_O-mt genes to other N-mt genes (Fig. 5), which is consistent
389 with a disproportionate role for N_O-mt genes in mitonuclear interactions.
390 Taken together, our data demonstrate strong selection against disassociation of
391 coevolved genes following hybridization, and conversely, strong selection for inter-
392 genomic compatibility within populations and species. These effects of mitonuclear
393 interactions are sufficiently strong in *T. californicus* that selection for rapid development
394 within a single generation identified key sites of mitonuclear interactions across the
395 genome. Mitonuclear coevolution in this species may be exceptionally strong (Burton et
396 al., 2006), but our results also suggest that even small numbers of mitonuclear
397 incompatibilities may result in large losses of fitness. Thus, the findings of the current
398 study are consistent with suggestions that inter-genomic incompatibilities may play a
399 significant role in establishing reproductive isolation between populations (Gershoni et
400 al., 2009; Hill, 2016, 2019). Finally, the potential strength of mitonuclear
401 incompatibilities, their polygenic nature, their range of impacts and their penetrance
402 supports calls for continued caution regarding human mitochondrial replacement therapy.
403 **Acknowledgments:**
404 The current study was funded by a National Science Foundation grant to RSB

(DEB1551466). The authors thank Drs. Felipe Barreto and Thiago Lima for advice regarding the sequencing methods and analyses, and Laura Furtado, Antonia Bock and Rebecca Pak for assistance with copepod culturing.

Author contributions:

T.M.H. and R.S.B. designed the experiments in the current study. T.M.H. performed the experiments and analyses, and R.S.B. conceived and supervised the study. T.M.H. prepared the figures, and T.M.H. and R.S.B. wrote the manuscript.

References:

Barreto, F. S. & Burton, R. S. Evidence for compensatory evolution of ribosomal proteins in response to rapid divergence of mitochondrial rRNA. *Mol. Biol. Evol.* **30**, 310-314 (2012).

Barreto, F. S., Watson, E. T., Lima, T. G., Willett, C. S., Edmands, S., Li, W. & Burton, R. S. Genomic signatures of mitonuclear coevolution across populations of *Tigriopus californicus*. *Nat. Ecol. Evol.* **2**, 1250-1257 (2018).

Bateson, W. Heredity and variation in modern lights. In *Darwin and Modern Science* (ed Seward, A. C.) (Cambridge University Press, 1909).

Burton, R. S. Genetic evidence for long term persistence of marine invertebrate populations in an ephemeral environment. *Evolution.* **51**, 993-998 (1997).

Burton, R. S. Hybrid breakdown in developmental time in the copepod *Tigriopus californicus*. *Evolution.* **44**, 1814-1822 (1990).

Burton, R. S. Mating system of the intertidal copepod *Tigriopus californicus*. *Mar. Biol.* **86**, 247-252 (1985).

Burton, R. S. & Barreto, F. S. A disproportionate role for mtDNA in Dobzhansky-Muller incompatibilities? *Mol. Ecol.* **21**, 4942-4957 (2012).

Burton, R. S., Ellison, C. K. & Harrison, J. S. The sorry state of F2 hybrids: consequences of rapid mitochondrial DNA evolution in allopatric populations. *Am. Nat.* **168**, 14-24 (2006).

Burton, R. S., Feldman, M. W. & Swisher, S. G. Linkage relationships among five enzyme-coding gene loci in the copepod *Tigriopus californicus*: a genetic confirmation of achiasmatic meiosis. *Biochem. Genet.* **19**, 1237-1245 (1981).

Burton, R. S. & Lee, B. N. Nuclear and mitochondrial gene genealogies and allozyme polymorphism across a major phylogeographic break in the copepod *Tigriopus californicus*. *Proc. Natl. Acad. Sci. USA.* **91**, 5197-5201 (1994).

Burton, R. S., Pereira, R. J. & Barreto, F. S. Cytonuclear genomic interactions and hybrid breakdown. *Annu. Rev. Ecol. Evol. Syst.* **44**, 281-302 (2013).

Dobzhansky, T. H. *Genetics and the Origin of Species* (Columbia University Press, 1937).

Edmands, S. Heterosis and outbreeding depression in interpopulation crosses spanning a wide range of divergence. *Evolution.* **53**, 1757-1768 (1999).

Edmands, S. Phylogeography of the intertidal copepod *Tigriopus californicus* reveals substantially reduced population differentiation at northern latitudes. *Mol. Ecol.* **10**, 1743-1750 (2001).

Ellison, C. K. & Burton, R. S. Disruption of mitochondrial function in interpopulation hybrids of *Tigriopus californicus*. *Evolution.* **60**, 1382-1391 (2006).

Ellison, C. K. & Burton, R. S. Genotype-dependent variation of mitochondrial transcriptional profiles in interpopulation hybrids. *Proc. Natl. Acad. Sci. USA.* **105**, 15831-15836 (2008).

Ellison, C. K. & Burton, R. S. Interpopulation hybrid breakdown maps to the mitochondrial genome. *Evolution.* **62**, 631-638 (2008b).

Eyre-Walker, A. Mitochondrial replacement therapy: are mito-nuclear interactions likely to be a problem? *Genetics.* **205**, 1365-1372 (2017).

Foley, B. R., Rose, C. G., Rundle, D. E., Leong, W. & Edmands, S. Postzygotic isolation involves strong mitochondrial and sex-specific effects in *Tigriopus californicus*, a species lacking heteromorphic sex chromosomes. *Heredity.* **111**, 391-401 (2013).

Ganz, H. H. & Burton, R. S. Genetic differentiation and reproductive incompatibility among Baja California populations of the copepod *Tigriopus californicus*. *Mar. Biol.* **123**, 821-827 (1995).

Gershoni, M., Templeton, A. R. & Mishmar, D. Mitochondrial bioenergetics as a major motive force of speciation. *Bioessays.* **31**, 642-650 (2009).

Harada, A. E., Healy, T. M. & Burton, R. S. Variation in thermal tolerance and its relationship to mitochondrial function across populations of *Tigriopus californicus*. *Front. Physiol.* **10**, 213 (2019). https://doi.org/10.3389/fphys.2019.00213.

Harrison, J. S. & Burton, R. S. Tracing hybrid incompatibilities to single amino acid substitutions. *Mol. Biol. Evol.* **23**, 559-564 (2005).

Hill, G. E. Mitonuclear coevolution as the genesis of speciation and the mitochondrial DNA barcode gap. *Ecol. Evol.* **6**, 5831-5842 (2016).

Hill, G. E. Mitonuclear ecology. *Mol. Biol. Evol.* **32**, 1917-1927 (2015).

Hill, G. E. Reconciling the mitonuclear compatibility species concept with rampant mitochondrial introgression. *Integr. Comp. Biol.* icz019 (2019). https://doi.org/10.1093/icb/icz019.

Hill, G. E., Havird, J. C., Sloan, D. B., Burton, R. S., Greening, C. & Dowling, D. K. Assessing the fitness consequences of mitonuclear interactions in natural populations. *Biol. Rev.* **94**, 1089-1104 (2018).

Kofler, R., Pandey, R. V. & Schlötterer, C. PoPoolation2: identifying differentiation between populations using sequencing of pooled DNA samples (Pool-Seq). *Bioinformatics.* **27**, 3435-3436 (2011).

Lane, N. *Power, Sex, Suicide: Mitochondria and the Meaning of Life* (Oxford University Press, 2005).

Levin, L., Blumberg, A., Barshad, G. & Mishmar, D. Mito-nuclear co-evolution: the positive and negative sides of functional ancient mutations. *Front. Genet.* **5**, 448. https://doi.org/10.3389/fgene.2014.00448.

Lima, T. G., Burton, R. S. & Willett, C. S. Genomic scans reveal multiple mito-nuclear incompatibilities in population crosses of the copepod *Tigriopus californicus*. *Evolution.* **73**, 609-620 (2019).

Lima, T. G. & Willett, C. S. Using Pool-seq to search for genomic regions affected by hybrid inviability in the copepod *T. californicus*. *J. Hered.* **109**, 469-476 (2018).

Meiklejohn, C. D., Holmbeck, M. A., Siddiq, M. A., Abt, D. N., Rand, D. M. & Montooth, K. L. An incompatibility between a mitochondrial tRNA and its nuclear-encoded tRNA synthetase compromises development and fitness in *Drosophila*. *PLoS Genet.* **9**, e1003238 (2013). https://doi.org/10.1371/journal.pgen.1003238.

Muller, H. J. Isolating mechanisms, evolution, and temperature. *Biol. Symp.* **6**, 71-125 (1942).

Pereira, R. J., Barreto, F. S., Pierce, N. T., Carneiro, M. & Burton, R. S. Transcriptome-wide patterns of divergence during allopatric evolution. *Mol. Ecol.* **25**, 1478-1493 (2016).

Peterson, D. L., Kubow, K. B., Connolly, M. J., Kaplan, L. R., Wetkowski, M. M.,

Leong, W., Phillips, B. C. & Edmands, S. Reproductive and phylogenetic divergence of tidepool copepod populations across a narrow geographical boundary in Baja California. *J. Biogeogr.* **40**, 1664-1675 (2013).

Li, H. & Durbin, R. Fast and accurate short read alignment with Burrows-Wheeler transform. *Bioinformatics.* **25**, 1754-1760 (2009).

Pritchard, V. L., Dimond, L., Harrison, J. S., Velázquez, C. C., Zieba, J. T., Burton, R. S. & Edmands, S. Interpopulation hybridization results in widespread viability selection across the genome in *Tigriopus californicus*. *BMC Genet.* **12**, 54 (2011). https://doi.org/10.1186/1471-2156-12-54.

Rand, D. M., Haney, R. A. & Fry, A. J. Cytonuclear coevolution: the genomics of cooperation. *Trends Ecol. Evol.* **19**, 645-653 (2004).

Rawson, P. D. & Burton, R. S. Functional coadaptation between cytochrome *c* and cytochrome *c* oxidase within allopatric populations of a marine copepod. *Proc. Natl. Acad. Sci. USA.* **99**, 12955-12958 (2002).

Reinhardt, K., Dowling, D. K. & Morrow, E. H. Mitochondrial replacement, evolution, and the clinic. *Science.* **341**, 1345-1346 (2013).

Sambrook, J. & Russell, D. W. Purification of nucleic acids by extraction with phenol:chloroform. *Cold Spring Harb. Protoc.* **2006**, pdb-rot4455 (2006). https://doi.org/10.1101/pdb.prot4455.

Sloan, D. B., Havird, J. C. & Sharbrough, J. The on-again, off-again relationship between mitochondrial genomes and species boundaries. *Mol. Ecol.* **26**, 2212-2236 (2017).

Tsuboko-Ishii, S. & Burton, R. S. Individual culturing of *Tigriopus* copepods and quantitative analysis of their mate-guarding behavior. *J. Vis. Exp.* **139**, e58378 (2018). https://doi.org/10.3791/58378.

Wallace, D. C. Bioenergetics, the origins of complexity, and the ascent of man. *Proc. Natl. Acad. Sci. USA.* **107**, 8947-8953 (2010a).

Wallace, D. C. Mitochondrial DNA mutations in disease and aging. *Environ. Mol. Mutagen.* **51**, 440-450 (2010b).

Willett, C. S. & Burton, R. S. Environmental influences on epistatic interactions: viabilities of cytochrome *c* genotypes in interpopulation crosses. *Evolution.* **57**, 2286-2292 (2003).

Willett, C. S. & Burton, R. S. Viability of cytochrome *c* genotypes depends on cytoplasmic backgrounds in *Tigriopus californicus*. *Evolution.* **55**, 1592-1599 (2001).

581 Willett, C. S., Lima, T. G., Kovaleva, I. & Hatfield, L. Chromosome-wide impacts on the
582 expression of incompatibilities in hybrids of *Tigriopus californicus*. *G3-Genes Genom.*
583 *Genet.* **6**, 1739-1749 (2016).
584

585 **Figure 1:**

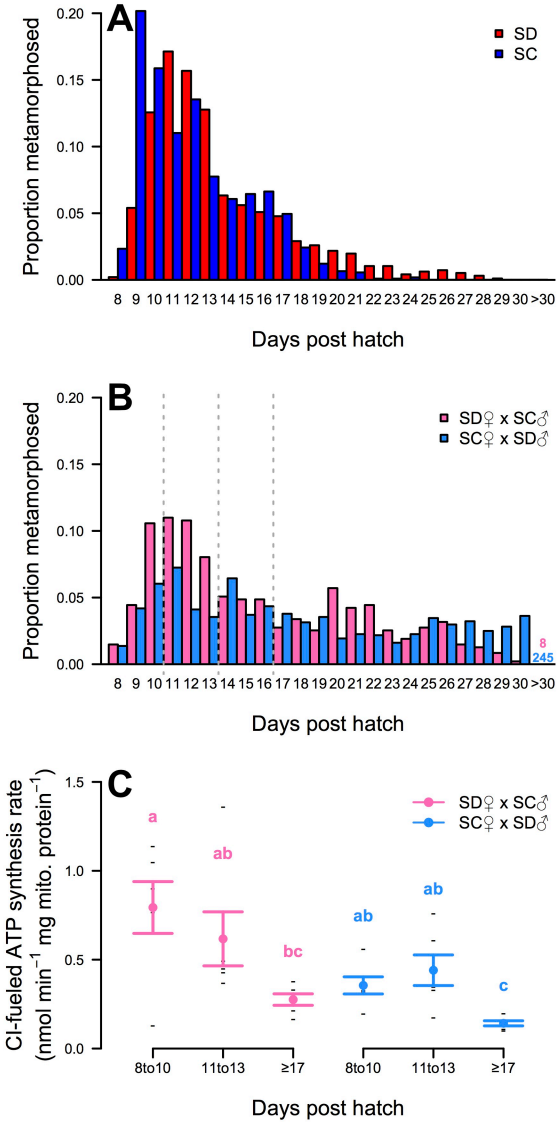

586 Fig. 1. Developmental time to metamorphosis for *T. californicus* nauplii as proportion of
587 individuals; A: SD (red; $N = 963$) and SC (blue; $N = 1,071$), and B: SD♀xSC♂ (pink; N
588 = 473) and SC♀xSD♂ (light blue; $N = 1,242$) F_2 hybrids. F_2 hybrids were split by
589 developmental time (dashed grey lines) and maximal complex I (CI)-fueled ATP
590 synthesis rates were measured for adults that metamorphosed 8-10, 11-13 and ≥17 dph
591 for both reciprocal crosses (C: mean ± s.e.m. for SD♀xSC♂ - pink and SC♀xSD♂ - light
592 blue; all measurements - black dashes; $N = 6$ per group). Shared lower case letters
593 indicate groups that do not differ significantly.

Figure 2:

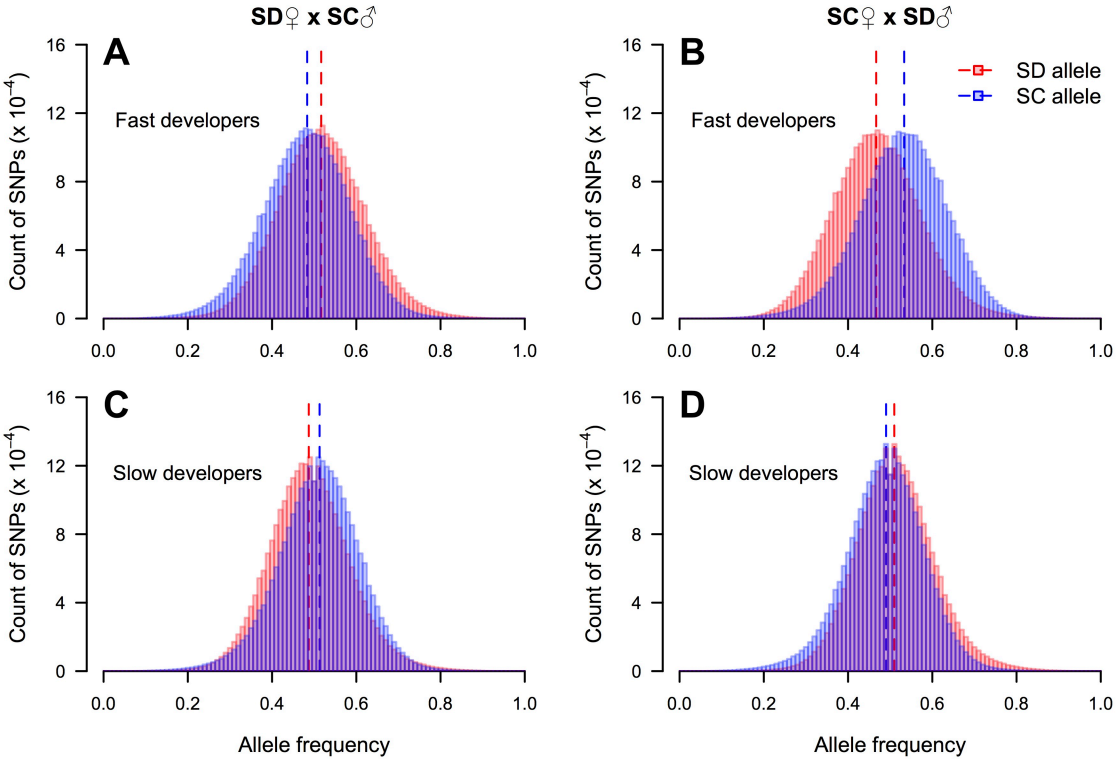

Fig. 2. Parental allele frequency histograms (SD - red and SC - blue) for all nuclear single nucleotide polymorphisms (SNPs; $N = 2{,}768{,}859$) in fast developing (A: SD♀xSC♂; B: SC♀xSD♂) and slow developing (C: SD♀xSC♂; D: SC♀xSD♂) reciprocal F_2 hybrids.

598 **Figure 3:**

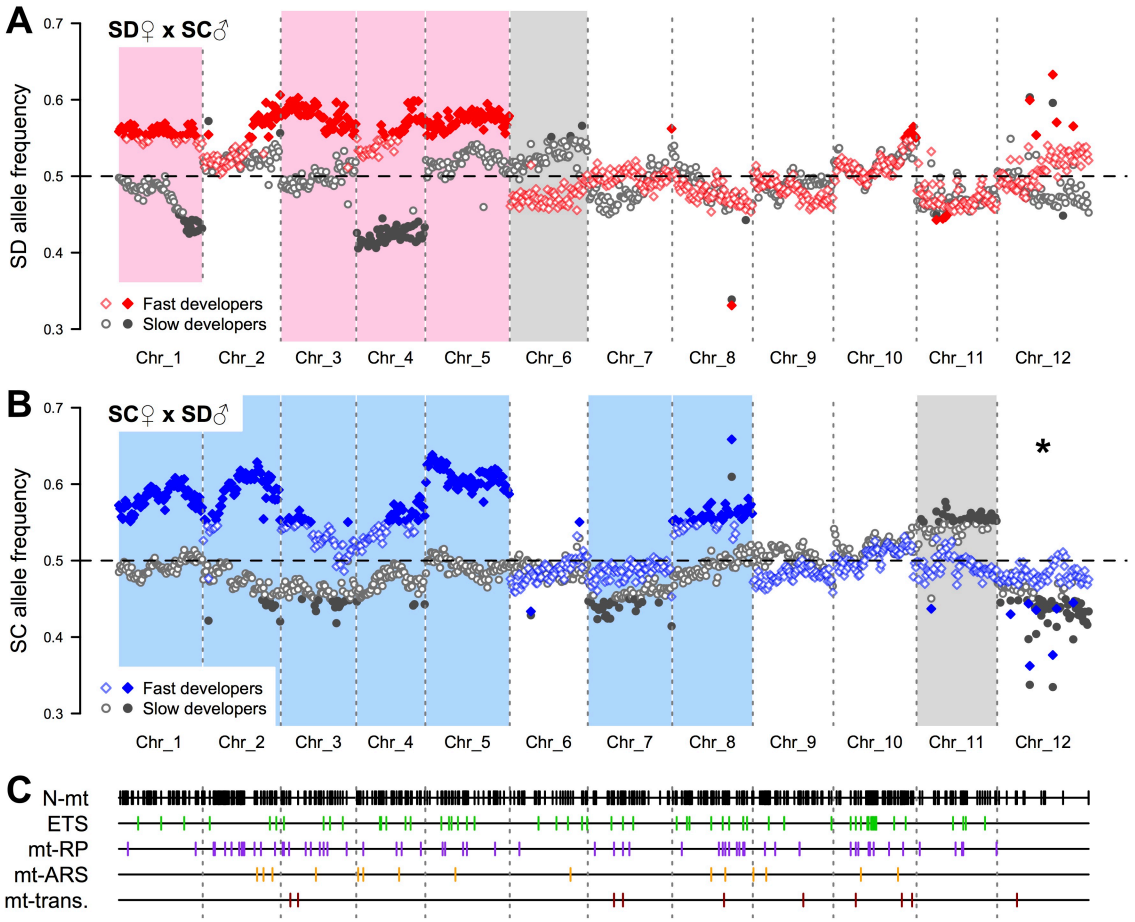

599 Fig. 3. Maternal allele frequencies in SD♀xSC♂ (A) and SC♀xSD♂ (B) fast (red or blue
600 diamonds) and slow (grey circles) developing F_2 hybrids. Shaded boxes indicate
601 chromosomes with significant deviations consistent with mitonuclear interactions (pink
602 and light blue - maternal bias in fast compared to slow developers; grey - maternal bias in
603 slow compared to fast developers). Filled symbols show allele frequency deviations
604 ≥0.05 from the expected value of 0.5. The asterisk indicates a significant difference in
605 allele frequencies between fast and slow developers that was unresolved by quantile
606 comparisons. Locations of 599 nuclear-encoded mitochondrial genes are displayed in
607 Panel C (all N-mt genes - black; classes of N_O-mt genes: electron transport system [ETS]
608 - green; ribosomal proteins [mt-RP] - purple; aminoacyl tRNA synthetases [mt-ARS] -
609 orange; transcription and DNA replication [mt-trans.] - dark red).
610

611 **Figure 4:**

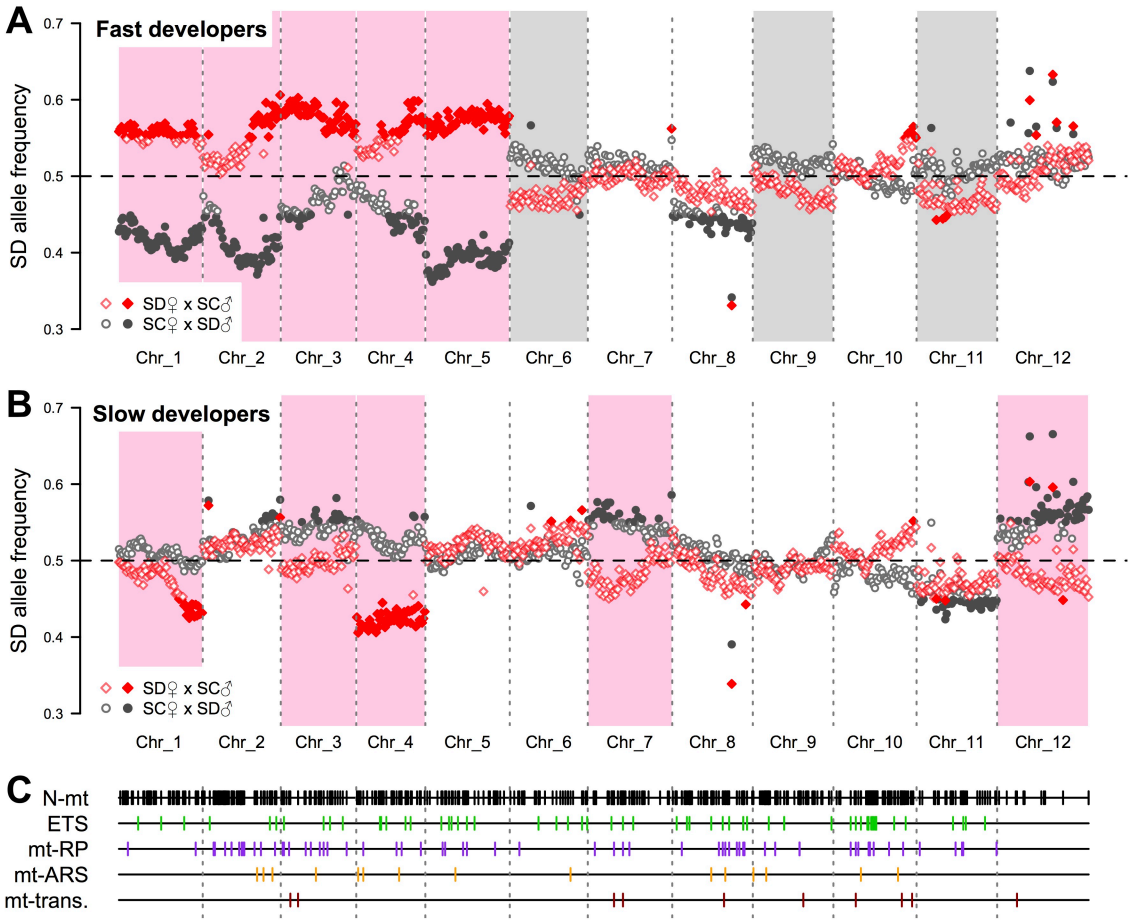

612 Fig. 4. SD allele frequencies in fast (A) and slow (B) developing SD♀xSC♂ (red
613 diamonds) and SC♀xSD♂ (grey circles) F_2 hybrids. Pink and grey shaded boxes indicate
614 chromosomes with significant deviations consistent with positive effects of mitonuclear
615 matching or mismatching, respectively, on developmental rate. Filled symbols show
616 allele frequency deviations ≥0.05 from the expected value of 0.5. Locations of 599
617 nuclear-encoded mitochondrial genes are display in Panel C (all N-mt genes - black;
618 classes of N_O-mt genes: electron transport system [ETS] - green; ribosomal proteins [mt-
619 RP] - purple; aminoacyl tRNA synthetases [mt-ARS] - orange; transcription and DNA
620 replication [mt-trans.] - dark red).

621 **Figure 5:**

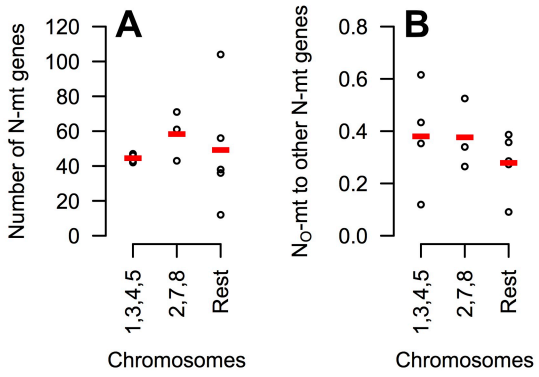

622 Fig. 5. Number of nuclear-encoded mitochondrial (N-mt) genes (A) and ratios of putative
623 interacting (N_O-mt genes) to other N-mt genes (B) for all twelve *T. californicus*
624 chromosomes. Chromosomes are grouped by those that were consistent with effects of
625 mitonuclear matching on development detected and resolved in both the SD♀xSC♂ and
626 SC♀xSD♂ crosses (1, 3, 4 and 5), in only the SC♀xSD♂ cross (2, 7 and 8), or in neither
627 of the crosses (6, 9, 10, 11 and 12): individual chromosome values - black circles; mean
628 values - red dashes.

Table 1: SD♀xSC♂ sequencing and allele frequency summary.

Chromosome	Number of 250kb windows	Number of SNPs	SNPs per window[1]	KS test *p*-value	Developmental time (dph)	Average coverage	SD allele frequency for 250 kb windows		
							μ	$q_{0.1}$	$q_{0.9}$
One	66	263,305	3989 ± 571	1.6×10^{-4} *	8-12	66X	0.555	0.546	0.565
					>22	77X	0.470	0.432	0.493
Two	61	221,662	3634 ± 920	0.58	8-12	66X	0.543	0.512	0.582
					>22	78X	0.523	0.512	0.535
Three	59	223,269	3784 ± 987	1.6×10^{-4} *	8-12	67X	0.578	0.560	0.596
					>22	78X	0.498	0.485	0.516
Four	54	205,183	3800 ± 928	5.8×10^{-4} *	8-12	66X	0.554	0.529	0.577
					>22	78X	0.423	0.412	0.435
Five	66	256,052	3880 ± 645	1.6×10^{-4} *	8-12	65X	0.573	0.560	0.584
					>22	76X	0.519	0.503	0.534
Six	61	223,748	3668 ± 1086	5.8×10^{-4} *	8-12	63X	0.473	0.460	0.487
					>22	76X	0.527	0.509	0.546
Seven	66	244,443	3703 ± 817	0.02	8-12	65X	0.499	0.488	0.510
					>22	76X	0.482	0.458	0.510
Eight	63	236,290	3750 ± 717	0.58	8-12	65X	0.475	0.462	0.495
					>22	77X	0.481	0.460	0.511
Nine	63	231,348	3672 ± 751	0.58	8-12	65X	0.481	0.462	0.500
					>22	77X	0.490	0.477	0.499
Ten	65	252,232	3880 ± 696	0.66	8-12	67X	0.516	0.497	0.549
					>22	79X	0.516	0.501	0.536
Eleven	63	225,229	3575 ± 837	0.66	8-12	65X	0.469	0.455	0.490
					>22	77X	0.470	0.458	0.485
Twelve	72	186,098	2585 ± 1360	6.2×10^{-3}	8-12	67X	0.514	0.486	0.538
					>22	78X	0.486	0.462	0.507

[1] μ ± σ; * significant after Bonferroni correction

Table 2: SC♀xSD♂ sequencing and allele frequency summary.

Chromosome	Number of 250kb windows	Number of SNPs	SNPs per window[1]	KS test *p*-value	Developmental time (dph)	Average coverage	SC allele frequency for 250 kb windows		
							μ	$q_{0.1}$	$q_{0.9}$
One	66	263,305	3989 ± 571	1.6×10^{-4} *	8-12	67X	0.582	0.563	0.598
					>22	80X	0.492	0.481	0.504
Two	61	221,662	3634 ± 920	5.8×10^{-4} *	8-12	67X	0.586	0.545	0.614
					>22	80X	0.470	0.448	0.493
Three	59	223,269	3784 ± 987	1.6×10^{-4} *	8-12	69X	0.533	0.505	0.553
					>22	81X	0.456	0.446	0.472
Four	54	205,183	3800 ± 928	5.8×10^{-4} *	8-12	68X	0.546	0.522	0.570
					>22	80X	0.471	0.454	0.489
Five	66	256,052	3880 ± 645	1.6×10^{-4} *	8-12	66X	0.609	0.593	0.627
					>22	78X	0.492	0.481	0.505
Six	61	223,748	3668 ± 1086	0.58	8-12	67X	0.486	0.468	0.505
					>22	78X	0.488	0.476	0.500
Seven	66	244,443	3703 ± 817	1.6×10^{-4} *	8-12	68X	0.486	0.472	0.498
					>22	80X	0.451	0.435	0.464
Eight	63	236,290	3750 ± 717	5.8×10^{-4} *	8-12	67X	0.556	0.542	0.570
					>22	79X	0.494	0.478	0.513
Nine	63	231,348	3672 ± 751	8.2×10^{-3}	8-12	68X	0.480	0.468	0.493
					>22	80X	0.503	0.487	0.518
Ten	65	252,232	3880 ± 696	0.09	8-12	69X	0.505	0.488	0.520
					>22	81X	0.516	0.496	0.532
Eleven	63	225,229	3575 ± 837	1.6×10^{-4} *	8-12	69X	0.493	0.480	0.508
					>22	79X	0.547	0.532	0.561
Twelve	72	186,098	2585 ± 1360	4.1×10^{-5} *	8-12	71X	0.475	0.465	0.498
					>22	83X	0.444	0.418	0.470

[1] μ ± σ; * significant after Bonferroni correction